Supporting Information

Ultrahigh energy storage properties with excellent stability in novel NaNbO₃-based lead-free ceramics with A-site vacancy: through Bi₂O₃ substitution strategy

Mingxing Zhou,[ab] Ruihong Liang,*[a] Zhiyong Zhou,[a] and Xianlin Dong*[ac]

[a] Key Laboratory of Inorganic Functional Materials and Devices, Shanghai Institute of Ceramics, Chinese Academy of Sciences, 588 Heshuo Road, Jiading District, Shanghai 201800, P. R. China

[b] University of Chinese Academy of Sciences, 19 Yuquan Road, Shijinshan District, Beijing 100049, P. R. China

[c] State Key Laboratory of High Performance Ceramics and Superfine Microstructure, Shanghai Institute of Ceramics, Chinese Academy of Sciences, 1295 Dingxi Road, Changning District, Shanghai 200050, P. R. China

*Corresponding Authors

E-mail: liangruihong@mail.sic.ac.cn; xldong@mail.sic.ac.cn

Experimental procedures

The ceramics of the $Na_{0.7}Bi_{0.1}NbO_3$ were prepared by conventional solid-state reaction with analytical pure starting chemicals of Na_2CO_3 (99.5%), Bi_2O_3 (99.99%), and Nb_2O_5 (99.93%). Raw materials were mixed and ball milled for 24 hours with ethyl alcohol as dispersant. After drying, the mixture was calcined 900 ℃ for 3 hours in air. The calcined powder was remixed, dried and then pressed into 13-mm diameter pellets under pressure of 120 MPa after adding polyvinyl alcohol (PVA) as organic binders. After burning off PVA at 800 ℃ for 2 hours in air, sintering was carried out at the temperature of 1150 ℃ for 2 hours. In order to minimize the evaporation of elemental Na during the process of sintering, the samples were buried into the corresponding calcined powders, and a double-crucible method was applied. The sintered pellets were polished to 0.2 ± 0.02 mm and coated with silver paste (the size of sliver electrode is 4.5 mm in diameter and corresponding area is 15.9 mm^2) in order to characterize electrical properties.

The crystal structure was examined by an X-ray diffraction (XRD, D/MAX-2550V; Rigaku, Tokyo, Japan) with a Cu Kα radiation. The surface morphology of the sample was investigated using a field emission scanning electron microscope (FESEM, Magellan400, FEI Company). Energy-dispersive X-ray spectroscopy (EDX) was collected from the attachment to the Magellan-400. The temperature dependence of dielectric constant (ε_r) and dielectric loss (tanδ) were measured by a precision impedance analyzer (E4980A; Agilent, Palo Alto, CA) with temperature-variable furnace over a temperature range from -50 to 160 ℃. Room temperature dielectric constant and tanδ were measured by a precision impedance analyzer (E4990A; Keysight, USA), which frequency range is from 20 Hz to 20 MHz. The DC breakdown strength measurement was performed using a Voltage-withstand testing device at room temperature. The unipolar polarization–electric field (*P–E*) hysteresis loops were measured by a commercial ferroelectric analyzer (TF Analyzer 2000, aixACCT, Aachen, Germany). The actual charge-discharge performance of the $Na_{0.7}Bi_{0.1}NbO_3$ ceramics were investigated via a charge-discharge platform with a specially designed,

high-speed capacitor discharge resistance, inductance, and capacitance load circuit (RLC) (Fig. S4).

Results and discussion

In order to investigate the relaxor behavior for $Na_{0.7}Bi_{0.1}NbO_3$ ceramics, the modified Curie-Weiss equation is given in upper-left corner of the Fig. S1. The value of $\gamma = 1$ indicates an ideal ferroelectric with a sharp phase transition, and it representing an obviously diffused transition with large deviation from the Curie-Wesis law when $\gamma = 2$. The plot of $\ln(1/\varepsilon - 1/\varepsilon_{max})$ as a function of $\ln(T\text{-}T_{max})$ for $Na_{0.7}Bi_{0.1}NbO_3$ ceramics at 100 kHz is displayed in Fig. S1 by linear fitting with Curie-Weiss equation to calculate the γ value. The data about 100 kHz were chose here to minimize any space charge contribution to the dielectric constant. The result is 1.86 for $Na_{0.7}Bi_{0.1}NbO_3$ ceramics, which indicates strong relaxation behavior. This phenomenon is attributed to the induced cation disorder due to the substitution of Bi^{3+} in A-site and formation of cationic vacancy.[1]
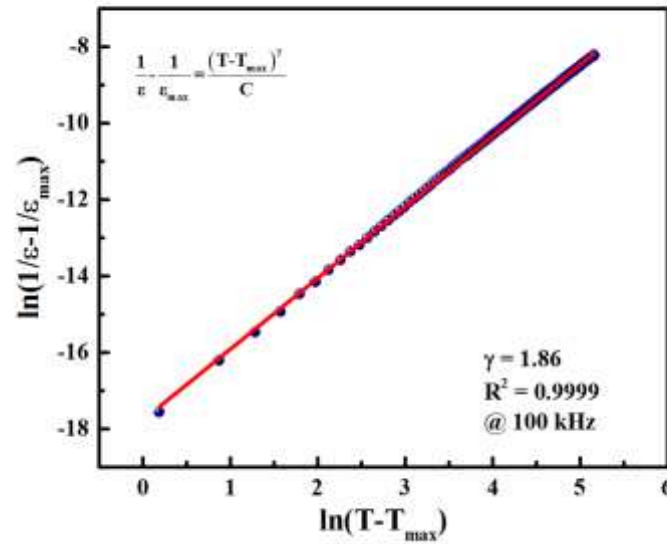
Fig. S1 Plots of $\ln(1/\varepsilon\text{-}1/\varepsilon_{max})$ versus $\ln(T\text{-}T_m)$ of the $Na_{0.7}Bi_{0.1}NbO_3$ ceramics.
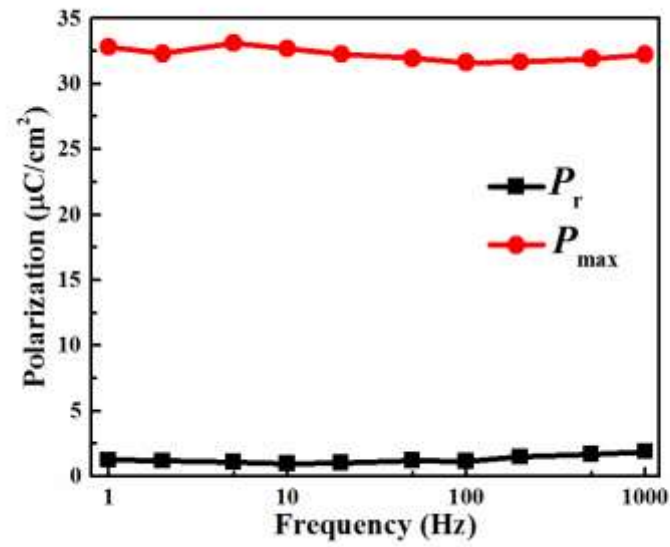
Fig. S2 Frequency dependence of P_{max} and P_r of the $Na_{0.7}Bi_{0.1}NbO_3$ ceramics.
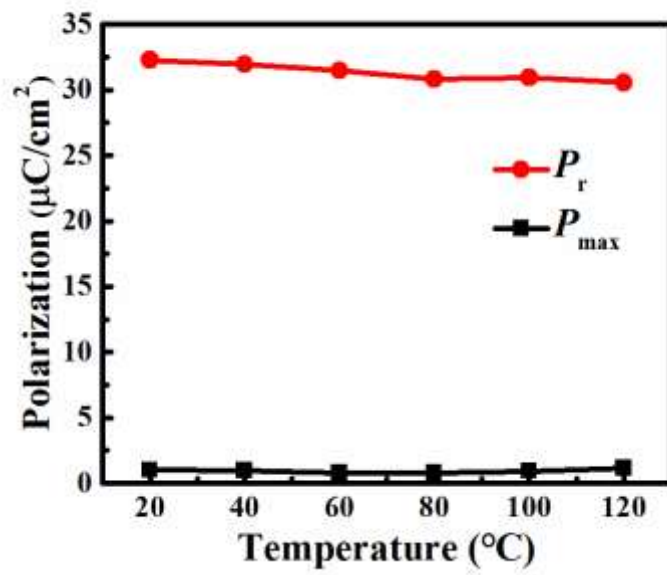
Fig. S3 Temperature dependence of P_{max} and P_r of the $Na_{0.7}Bi_{0.1}NbO_3$ ceramics.
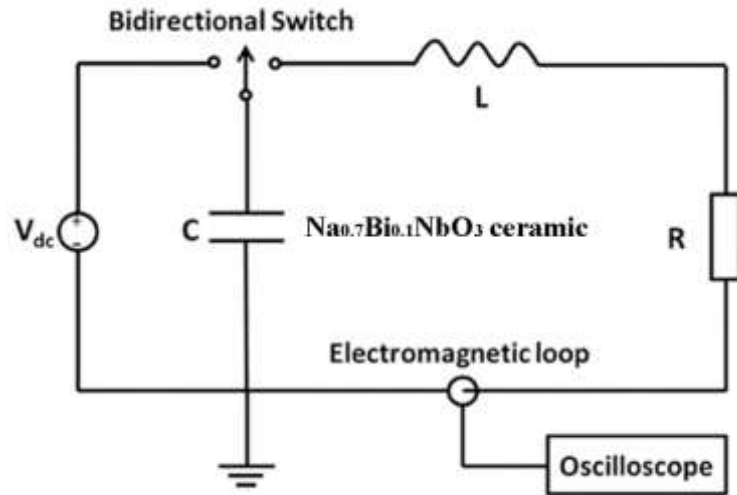
Fig. S4 Schematic diagram of the charging-discharging cycle measuring system.

Table S1 compares the pulsed charge-discharge performance of the $Na_{0.7}Bi_{0.1}NbO_3$ ceramics with those of recently reported systems. The ultrahigh values of C_D and P_D of the here present $Na_{0.7}Bi_{0.1}NbO_3$ ceramics are superior to those of BNT-based ceramics, which currently present the best lead-free material, and obviously larger than those of other commercial lead-based anti-ferroelectric ceramics (mostly $P_D < 10$ MW/cm^3, Table S1) [2-9]

Table S1. Comparison of the charge-discharge properties of the $Na_{0.7}Bi_{0.1}NbO_3$ ceramics and other reported ceramics.

Composition	E(kV/mm)	$t_{0.90}$(µs)	C_D(A/cm^2)	P_D(MW/cm^3)	Ref
$Pb_{0.90}La_{0.04}Ba_{0.04}(Zr_{0.616}Sn_{0.264}Ti_{0.12})O_3$	6.67	~1	~242	~1.95	[7]
$Pb_{0.925}La_{0.05}(Zr_{0.42}Sn_{0.40}Ti_{0.18})O_3$	3.5	~0.065	~183	~3.2	[5]
$Pb_{0.93}La_{0.04}Nb_{0.02}(Zr_{0.42}Sn_{0.40}Ti_{0.18})_{0.98}O_3$	4.0	~0.500	~143	~2.9	[6]
$Pb_{0.87}Ba_{0.1}La_{0.2}(Zr_{0.6}Ti_{0.07}Sn_{0.33})O_3$	6.0	/	~223	~6.69	[2]
$Pb_{0.98}La_{0.02}(Zr_{0.35}Sn_{0.55}Ti_{0.10})_{0.995}O_3$	8.2	/	~438	~18.0	[9]
BNT-BT-0.32SBT	6.0	~0.675	~400	~12.0	[2]
$Na_{0.7}Bi_{0.1}NbO_3$	10.0	~0.155	~1250	~62.5	This work

References:

[1]   J. Wu, A. Mahajan, L. Riekehr, H. Zhang, B. Yang, N. Meng, Z. Zhang, H. Yan, *Nano. Energy.,* 2018, **50**, 723.

[2]   F. Li, K. Yang, X. Liu, J. Zou, J. Zhai, B. Shen, P. Li, J. Shen, B. Liu, P. Chen, *Scripta. Mater.,* 2017, **141**, 15.

[3]   R. Xu, Z. Xu, Y. Feng, X. Wei, J. Tian, *J. Appl. Phys.,* 2016, **120**, 144102.

[4]   R. Xu, Z. Xu, Y. Feng, H. He, J. Tian, K. Yu, *Ceram. Int.,* 2016, **42**, 9094.

[5]   H. Zhang, X. Chen, F. Cao, G. Wang, X. Dong, Z. Hu, T. Du, *J. Am. Ceram. Soc.,* 2010, **93**, 4015.

[6]   X. Chen, H. Zhang, F. Cao, G. Wang, X. Dong, Y. Gu, H. He, Y. Liu, *J. Appl. Phys.,* 2009, **106**, 034105.

[7]   R. Xu, Z. Xu, Y. Feng, H. He, J. Tian, D. Huang, *J. Am. Ceram. Soc.,* 2016, **99**, 2984.

[8]   C. Xu, Z. Liu, X. Chen, S. Yan, F. Cao, X. Dong, G. Wang, *AIP Adv.,* 2017, **7**, 115108.

[9]   C. Xu, Z. Liu, X. Chen, S. Yan, F. Cao, X. Dong, G. Wang, *J. Appl. Phys.,* 2016, **120**, 074107.